Hypoglycaemia, liver necrosis and perinatal death in mice lacking all isoforms of phosphoinositide 3-kinase p85α

David A. Fruman[1], Franck Mauvais-Jarvis[2], Daniel A. Pollard[1], Claudine M. Yballe[1], Derek Brazil[2], Roderick T. Bronson[3], C. Ronald Kahn[2] & Lewis C. Cantley[1]

Phosphoinositide 3-kinases produce 3′-phosphorylated phosphoinositides that act as second messengers to recruit other signalling proteins to the membrane[1]. Pi3ks are activated by many extracellular stimuli and have been implicated in a variety of cellular responses[1]. The Pi3k gene family is complex and the physiological roles of different classes and isoforms are not clear. The gene *Pik3r1* encodes three proteins (p85α, p55α and p50α) that serve as regulatory subunits of class I_A Pi3ks (ref. 2). Mice lacking only the p85α isoform are viable but display hypoglycaemia and increased insulin sensitivity correlating with upregulation of the p55α and p50α variants[3]. Here we report that loss of all protein products of *Pik3r1* results in perinatal lethality. We observed, among other abnormalities, extensive hepatocyte necrosis and chylous ascites. We also noted enlarged skeletal muscle fibres, brown fat necrosis and calcification of cardiac tissue. In liver and muscle, loss of the major regulatory isoform caused a great decrease in expression and activity of class I_A Pi3k catalytic subunits; nevertheless, homozygous mice still displayed hypoglycaemia, lower insulin levels and increased glucose tolerance. Our findings reveal that p55α and/or p50α are required for survival, but not for development of hypoglycaemia, in mice lacking p85α.

Class I_A Pi3ks are heterodimers of a catalytic subunit and a regulatory subunit. These enzymes respond to tyrosine-kinase–based signals by moving from the cytoplasm to cellular membranes, primarily through interactions of the regulatory subunit with activated signalling complexes. Three genes encoding catalytic subunits (p110α, p110β and p110δ) and three encoding regulatory subunits (p85α, p85β and p55γ) have been identified in mammals. The gene encoding p85α (*Pik3r1*) also encodes two smaller variants, p55α (also called AS53) and p50α (refs 4–6).

Mice lacking *Pik3r1* protein products die perinatally[7]. On the basis of expected mendelian frequencies, in a mixed genetic background (129SvEv×C57Bl/6) or an inbred 129SvEv background only approximately 5% of *Pik3r1*$^{-/-}$ mice were alive at 5–10 days of age (Table 1). At 2–4 days of age, the percentage of viable homozygous animals was less than 35% (Table 1). We found the expected number of viable homozygous embryos until day 18.5 (approximately one day before birth), at which time there was a small decline (Table 1). Thus, mutant mice die either late in gestation or in the first ten days after birth. Breeding the *Pik3r1* mutation into a more outbred background increased the frequency of surviving homozygotes to approximately 30% after one week (Table 1). Some animals survived for 3–7 weeks and were of normal size and appearance.

To determine the cause of perinatal lethality in *Pik3r1*$^{-/-}$ mice, we stained tissue sections with haematoxylin and eosin (H&E). Three of 16 embryos at day 18.5 (129×B6) and 6 of 19 neonates (various backgrounds) had livers with areas of necrosis (Fig. 1*a*,*b*). At higher magnification the necrosis appeared to be confined to

Table 1 • Genotypes of progeny of *Pik3r1*$^{+/-}$ intercrosses

	Pik3r1$^{+/+}$	*Pik3r1*$^{+/-}$	*Pik3r1*$^{-/-}$
Genetic background	genotype determined at day 5–10 postnatal		
129×B6 mixed	95	187	4
129 inbred	24	25	1
outbred,			
1 generation	23	44	6
2 generation	78	152	17
3 generation	15	41	7
	genotype at 2–4 days		
129×B6	17	35	6
	genotype of embryos (129×B6)		
Gestation age			
E15.5	21	47	17
E17.5	9	21	14
E18.5	25	36	15
	genotype of embryos (129 inbred)		
E16.5	6	14	5
E18.5	7	9	5

E, embryonic day.

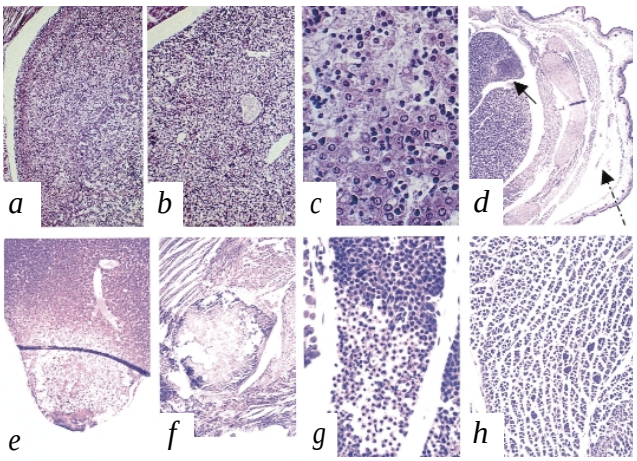

Fig. 1 Histopathology in *Pik3r1*$^{-/-}$ mice. Sections were stained with haematoxylin and eosin. ***a***, Region of necrosis in liver of day 18.5 embryo. Magnification, ×25. ***b***, Liver of wild-type day 18.5 embryo. Magnification, ×25. ***c***, Higher magnification (×100) of border between necrotic and living tissue. Note the intact nuclei (clear round structures) in healthy hepatocytes and the nearly complete absence of nuclei from paler staining necrotic hepatocytes. ***d***, Liver necrosis (filled arrow) and oedema (dashed arrow) in dead newborn. Magnification, ×10. ***e***, Effaced region of liver of 12-day-old animal. The purple line is an artefact of slide preparation. Magnification, ×50. ***f***, Unusual nodule in heart of 26-day-old animal. Magnification, ×25. ***g***, Necrosis in brown adipocyte tissue of dead newborn. Magnification, ×100. ***h***, Sporadic enlarged skeletal muscle fibres in dead newborn. Magnification, ×50.

[1]*Division of Signal Transduction, Beth Israel Deaconess Medical Center and Department of Cell Biology, Harvard Medical School, Boston, Massachusetts, USA.* [2]*Research Division, Joslin Diabetes Center, and Department of Medicine, Harvard Medical School, Boston, Massachusetts, USA.* [3]*Tufts School of Veterinary Medicine, Boston, Massachusetts, USA. Correspondence should be addressed to L.C.C. (e-mail: cantley@helix.mgh.harvard.edu).*

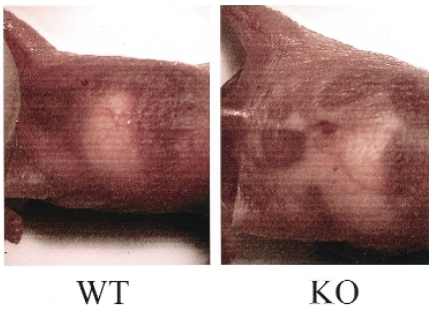

Fig. 2 Chylous ascites in a 3-day-old *Pik3r1*$^{-/-}$ mouse. A wild-type pup is shown for comparison to point out the normal white appearance of the stomach after nursing. In contrast, the fluid in the mutant animal extends throughout the peritoneal space.

the hepatocytes and did not affect the haematopoietic cells (Fig. 1*c*). Many of the embryos also showed subcutaneous oedema (Fig. 1*d*). The absence of nuclei or nuclear fragments from most of the hepatocytes is consistent with death by necrosis, not apoptosis. TUNEL staining of liver sections showed the presence of apoptotic cells primarily at the periphery of the lesions (data not shown). This phenotype is distinct temporally and histologically from liver degeneration associated with disruption of genes encoding certain components of the NF-κB signalling pathway[8,9].

Some outbred animals survived liver damage, as evidenced by mineralized areas in the livers of older mice (Fig. 1*e*). Nevertheless, ongoing hepatic injury was suggested by elevated serum transaminases in two of six animals. There was a consistent decrease in albumin (2.4 versus 3.7, $P<0.05$) and total protein in the serum (3.7 versus 5.1, $P<0.05$) of older animals, irrespective of transaminase levels. Pi3k has been implicated in the trafficking of bile acid transporters[10,11]; however, serum bilirubin levels were normal. It is possible that loss of *Pik3r1* disrupts other critical transport processes in hepatocytes[10,12].

Most of the homozygous animals of all genetic backgrounds showed the presence of chylous ascites (Fig. 2). In some animals, the ascites comprised more than 10% of their body weight. Microscopic analysis of the fluid confirmed the presence of fat droplets, and lipid analysis showed a high concentration of triglycerides (3.0±0.5 mg/ml, n=4), consistent with a chylous effusion. Chylous ascites usually indicates obstruction of the lymphatic vessels leading to the thoracic duct, most commonly caused by neoplasia[13]. In newborn mice it is more likely to be caused by a congenital malformation of the intestinal lymphatics[13]. The homozygous animals that were alive at weaning appeared to have cleared the fluid. Three older outbred mice that showed difficulty breathing were sacrificed and found to have a clear pleural effusion.

The hearts of two animals showed round nodules that appeared to be calcified as judged by dark purple staining (haematoxylin; Fig. 1*f*), and two animals had extensive necrosis of brown fat cells (Fig. 1*g*). This suggests that necrosis might not be confined to the liver. Another histological abnormality in many homozygotes was the presence of enlarged skeletal muscle fibres (Fig. 1*h*). The diameter of these fibres was at least twice the diameter of the surrounding fibres. This finding is surprising in light of the observation that constitutively active Pi3k enhances myoblast differentiation and increases myotube size *in vitro*[14]. Moreover, active p110 increases the size of cardiac myocytes in transgenic mice[15]. These results could be consistent with p85α restricting Pi3k activation during muscle development.

Pi3k is essential for many cellular responses to insulin[16]. Class I_A Pi3k is recruited to tyrosine-phosphorylated insulin receptor substrates (IRS proteins) through SH2 domains in the regulatory subunit[17], but individual class I_A regulatory isoforms may function differently during responses to insulin[6,18]. In hyperglycaemic, obese mice (strain ob/ob), p85α expression in the liver is reduced, whereas p55α and p50α are upregulated[19]. By contrast, mice genetically lacking only the p85α isoform show upregulation of p50α and p55α, but this was associated with hypoglycaemia and increased insulin sensitivity[3]. We found that mice lacking all isoforms of *Pik3r1* also showed hypoglycaemia and lower insulin levels, both in fasting and random-fed states, compared with wild-type littermates (Fig. 3*a*). In addition, they showed a greater ability to dispose of a glucose load and they maintained lower insulin levels during an intraperitoneal glucose tolerance test (Fig. 3*b*). Expression of the glucose transporter proteins Glut1 and Glut4 was similar in skeletal muscle of wild-type and mutant mice (Fig. 3*c*). Although hepatocyte necrosis may reduce gluconeogenesis and contribute to hypoglycaemia, we observed lower fasted and fed glucose levels in more than 95% of animals, whereas we found evidence for liver injury in only approximately 33%.

We assessed class I_A Pi3k expression and insulin-stimulated responses in liver and skeletal muscle. Loss of *Pik3r1* expression (Figs 3*c* and 4*a*) in homozygous tissues was associated with an 80–90% reduction in total class I_A Pi3k activity as detected in pan-p85 immunoprecipitates (Fig. 4*b*). The expression and activity of

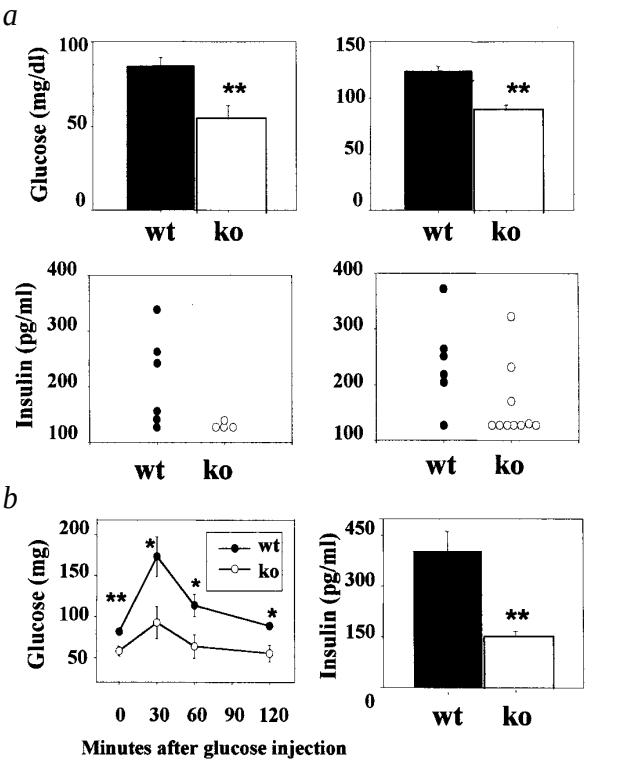

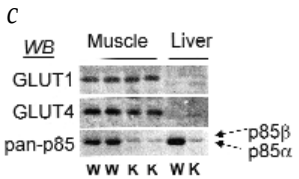

Fig. 3 Lower glucose and insulin concentrations in *Pik3r1*$^{-/-}$ mice. ***a***, We determined fasting glucose (top left) and insulin (bottom left) concentrations as well as random fed glucose (top right) and insulin (bottom right) concentrations by tail bleeding in 2–3-week *Pik3r1*$^{-/-}$ and wild-type (WT) mice. Values for glucose levels represent the mean±s.e.m. of n=6–17 mice per genotype. $^{**}P<0.01$ *Pik3r1*$^{-/-}$ versus wild type. Insulin concentrations determined by ELISA are shown in a scatter plot. ***b***, We performed an i.p. GTT (2g/kg) on overnight fasted 3-week *Pik3r1*$^{-/-}$ and wild-type mice. We measured glucose concentrations (left) by tail bleeding at the indicated time points. We determined insulin concentrations (right) 60 min after glucose injection by ELISA. Values represent the mean±s.e.m. of n=6 mice per genotype. $^{*}P<0.05$, $^{**}P<0.01$ *Pik3r1*$^{-/-}$ versus wild type. ***c***, We immunoblotted GLUT1 and GLUT4 from muscle of 4-week wild-type (W) and mutant (K) animals on parallel filters prepared from the same tissue extracts. Liver served as a negative control. We probed the upper portion of one filter with pan-p85 antibody, which recognizes a doublet of p85α and p85β.

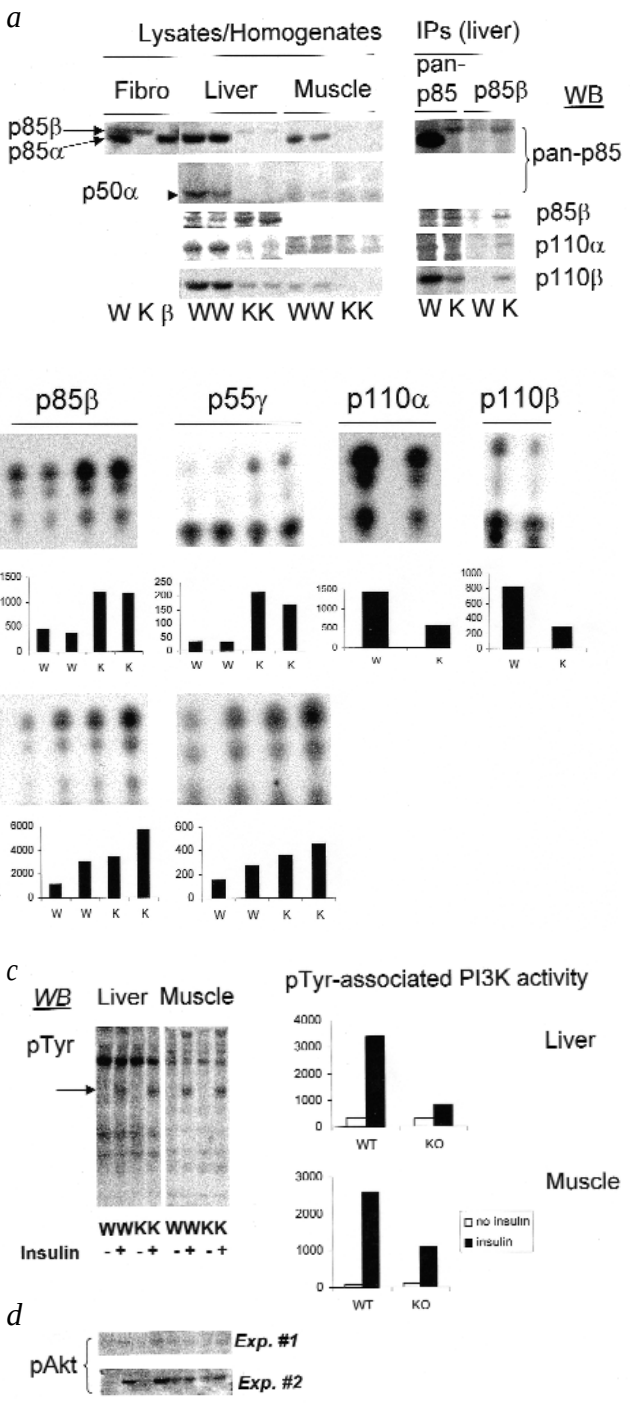

Fig. 4 Biochemical analysis of Pi3k expression and activity in insulin-responsive tissues. ***a***, Left, we immunoblotted lysates from fibroblasts or homogenates from liver or muscle with specific antibodies recognizing the indicated Pi3k isoforms. Right, we immunoprecipitated liver homogenates with pan-p85 or a p85β-specific antiserum and immunoblotted with the indicated antibodies. W, wild-type; K, mutant (*Pik3r1*$^{-/-}$); β, p85β mutant (*Pik3r2*$^{-/-}$). ***b***, We immunoprecipitated liver (top) and muscle (bottom) homogenates with the indicated antibodies, and measured Pi3k activity using PtdIns, PtdIns-4-P and PtdIns-4,5-P_2 as substrates. We stopped reactions after 5 min for pan-p85 immunoprecipitates and after 15 min for other samples. We quantitated the radioactivity in each PtdIns-3-phosphate spot (top arrow) by Phosphorimager and graphed the data (in arbitrary units, note the differences in scale) below the thin layer chromatograms. ***c***, Effects of insulin treatment on total tyrosine phosphorylation and pTyr-associated Pi3k. We fasted animals overnight and injected them intravenously with insulin or its diluent; then we removed the livers after 4 min and muscle after 6-8 min. Left, we immunoblotted homogenates of liver and muscle with anti-pTyr antibody. The arrow indicates a 90-kD band that probably represents the tyrosine-phosphorylated, activated insulin receptor. Right, Pi3k activity in anti-pTyr immunoprecipitates from liver and muscle. The graphs depict the average of pTyr-associated activity in 2–4 animals of each genotype and condition. ***d***, Phosphorylation of serine 473 of Akt. The same homogenates used for the anti-pTyr blot above (Exp. #1) or from a different set of mice (Exp. #2) were immunoblotted with anti-pSer473Akt.

p110α and p110β were also reduced (Fig. 4*a*,*b*). This result is consistent with a previous report that catalytic isoforms may be degraded when regulatory subunits are limiting[20]. Pi3k activity in anti-phosphotyrosine (pTyr) immunoprecipitates was reduced on average by 70% in liver and 55% in muscle compared with wild type (Fig. 4*c*). p85β expression was increased, especially in the liver, and the amount of p110 and Pi3k activity associated with this isoform were augmented by two- to threefold (Fig. 4*a*,*b*). The p55γ regulatory subunit is primarily expressed in brain and testis[21], and little activity was associated with this isoform in wild-type liver or muscle. We detected a small increase of activity in p55γ immunoprecipitates from homozygous tissues (Fig. 4*b*).

The production of 3′-phosphorylated phosphoinositides by activated Pi3k leads to phosphorylation and activation of the serine/threonine kinase Akt (also known as PKB; ref. 22). Insulin treatment caused comparable increases in phosphorylation of Akt in liver and muscle of wild-type and mutant animals (Fig. 4*d*). The *in vitro* kinase activity of Akt increased by twofold in livers of insulin-treated animals of both genotypes (data not shown). Thus, Akt activation was not diminished despite reduced Pi3k activity associated with tyrosine-phosphoproteins. Others have reported that Akt activation does not necessarily correlate with the amount of Pi3k recruited to tyrosine-phosphorylated proteins following insulin treatment[23,24].

Mice deficient in the insulin receptor or Irs proteins develop hyperglycaemia and glucose intolerance[25,26]. Hypoglycaemia and increased glucose disposal in mice lacking p85α have been shown, although insulin-dependent Pi3k activation was augmented due to an isoform switch to p55α and p50α (ref. 3). Together with extensive insulin signalling studies *in vitro*[16], these data supported the prediction that *Pik3r1*$^{-/-}$ mice would exhibit evidence of insulin resistance. However, our results show that the mice are hypoglycaemic and display increased glucose tolerance. The early lethality precluded detailed measurements of insulin sensitivity in target tissues. Although increased insulin sensitivity is not the only possible mechanism to explain the phenotype, it is apparent nevertheless that a great reduction in class I_A Pi3k function does not cause insulin resistance. Of note, increased class I_A Pi3k function causes partial insulin resistance in 3T3-L1 adipocytes[27].

Methods

Mice. Mice were maintained and studied according to institutional guidelines. We generated mice (strain 129×B6) with a germline disruption of *Pik3r1* as described[7]. We tranferred the mutation to the inbred 129SvEv background in a single cross by mating the founder chimaeric males with wild-type 129SvEv females. We generated outbred mice carrying the mutation by breeding heterozygous animals (129×B6) with wild-type ICR and Swiss-Webster mice (Taconic). We used different wild-type animals for subsequent generations of outbreeding. ((129×B6)×ICR) heterozygotes were mated with ((129×B6) ×Swiss-Webster) heterozygotes to test for survival of homozygotes after successive rounds of outbreeding. Mice were housed in a

barrier facility in microisolator cages. Though *Pik3r1* is required for normal B-cell development and proliferation[7], we detected no signs of infection even in moribund homozygotes. We genotyped animals by PCR as described[7].

Metabolic studies. For glucose tolerance tests (GTT) and random-fed blood glucose, we took blood samples from mouse tails using heparinized microcapillaries and extracted plasma. For GTT, we obtained blood samples at 0, 30, 60 and 120 min after intraperitoneal (i.p.) injection of dextrose (2 g/kg). We determined blood glucose values from whole venous blood using an automatic glucose monitor (One Touch II, Lifescan). We measured insulin levels in plasma by ELISA using mouse insulin as a standard (Crystal Chem).

Antibodies. We purchased rabbit anti-(pan)p85 (Upstate Biotechnology), which recognizes all variants of p85α and p85β, rabbit antibodies H-201 and S-19 specific for p110α and p110β (SantaCruz Biotechnology), rabbit anti-GLUT-1 and anti-GLUT4 (Chemicon International) and HRP-coupled secondary antibodies (Boehringer). We raised rabbit anti-p55γ against aa 8–24 of the mouse protein, and rabbit anti-p85β as described[7]. Anti-pTyr was provided by T. Roberts.

In vivo insulin stimulation. We fasted mice overnight and anaesthetized them with 2,2,2-tribromoethanol injected i.p. After mice had lost pedal and corneal reflexes, we injected regular human insulin (5 U) or its diluent into the inferior vena cava. We removed the liver and limb muscle at 4 min and 6–8 min after injection, respectively, and froze the tissues in liquid nitrogen.

Biochemical analysis of tissue homogenates. We minced frozen liver and muscle with a razor blade then homogenized the samples in a Dounce apparatus (liver) or a Tissumizer (muscle) in 5 ml buffer A (50 mM Hepes, pH 7.4, 10% Triton X-100, 50 mM sodium pyrophosphate, 100 mM NaF, 10 mM EDTA, 10 mM Na_3VO_4, 2 mM benzamidine, and leupeptin, aprotinin, AEBSF (10 μg/ml each)). We left the samples on ice for 30 min then centrifuged at 3,000 r.p.m. for 15 min in a table-top Sorvall to pellet unbroken cells and tissue clumps. We removed the supernatants and centrifuged in a Ti70.1 rotor at 55,000 r.p.m. for 1 h at 4 °C. We removed the fat layer from the surface and the transferred the remaining supernatants to fresh tubes on ice. We determined protein concentrations using the Biorad protein assay reagent. For immunoblotting, we boiled protein (200 μg) in SDS–PAGE sample buffer. For Pi3k assays, we diluted 1 mg protein to 800 μl with fresh buffer A and subjected the lysates to immunoprecipitation with the indicated antibodies. For immunoblotting of immunoprecipitates, we diluted 5 mg protein to 1 ml with buffer A and pre-cleared with 60 μl protein A–Sepharose (50% slurry) for 1–2 h at 4 °C. We pelleted the beads by a brief centrifugation, transferred the supernatants to fresh tubes, and added immunoprecipitating antibodies at 5× the amount used for Pi3k assays. We left the samples rocking overnight at 4 °C, then added protein A–Sepharose slurry (30 μl for Pi3k assay tubes and 80 μl for immunoblotting tubes) and rocked for an additional 1–2 h. We pelleted the beads and washed three times with buffer B (50 mM Hepes, pH 7.4, 0.5 M NaCl, 10% Triton X-100, 10 mM EDTA, 10 mM Na_3VO_4, and leupeptin, aprotinin, AEBSF (10 μg/ml each)) and twice with buffer C (25 mM Tris, pH 7.2, 137 mM NaCl). We boiled samples for immunoblotting in SDS–PAGE sample buffer. We transferred SDS–PAGE gels electrophoretically to nitrocellulose membranes and immunoblotted using standard procedures with ECL detection. We performed Pi3k assays as described[28] using a mixture of phosphatidylinositol (PtdIns), PtdIns-4-phosphate and PtdIns-4,5-bisphosphate and phosphatidylserine as carrier. We separated ^{32}P-labelled lipids by TLC and visualized using a Phosphorimager (BioRad) and autoradiographic film.

Histology. We fixed embryos and tissue samples in Bouin's solution and embedded them in paraffin. We stained sections with H&E or processed them for TUNEL assay using a kit (Boehringer).

Acknowledgements

We thank H. Warren and E. Meluleni for help with necropsy and histopathology; J. Alvarez for lipid analysis; M. White for the anti-p55γ antibody; T. Roberts for the anti-pTyr antibody; and I. Arias, S. Snapper, B. Sleckman, S. Thomas, M. Wahl and members of the Cantley and Kahn labs for helpful suggestions. D.A.F. was supported by fellowships from the Damon Runyan-Walter Winchell Cancer Research Fund and the Leukemia Society of America. This work was supported by NIH grants GM41890 to L.C.C. and DK55545 to C.R.K.

Received 17 November; accepted 16 July 2000.

1. Vanhaesebroeck, B. & Waterfield, M.D. Signaling by distinct classes of phosphoinositide 3-kinases. *Exp. Cell Res.* **253**, 239–254 (2000).
2. Fruman, D.A., Meyers, R.E. & Cantley, L.C. Phosphoinositide kinases. *Annu. Rev. Biochem.* **67**, 481–507 (1998).
3. Terauchi, Y. *et al.* Increased insulin sensitivity and hypoglycaemia in mice lacking the p85 α subunit of phosphoinositide 3-kinase. *Nature Genet.* **21**, 230–235 (1999).
4. Fruman, D.A., Cantley, L.C. & Carpenter, C.L. Structural organization and alternative splicing of the murine phosphoinositide 3-kinase p85 α gene. *Genomics* **37**, 113–121 (1996).
5. Antonetti, D.A., Algenstaedt, P. & Kahn, C.R. Insulin receptor substrate 1 binds two novel splice variants of the regulatory subunit of phosphatidylinositol 3-kinase in muscle and brain. *Mol. Cell. Biol.* **16**, 2195–2203 (1996).
6. Inukai, K. *et al.* p85α gene generates three isoforms of regulatory subunit for phosphatidylinositol 3-kinase (PI 3-kinase), p50α, p55α, and p85α, with different PI 3-kinase activity elevating responses to insulin. *J. Biol. Chem.* **272**, 7873–7882 (1997).
7. Fruman, D.A. *et al.* Impaired B cell development and proliferation in absence of phosphoinositide 3-kinase p85α. *Science* **283**, 393–397 (1999).
8. Beg, A.A., Sha, W.C., Bronson, R.T., Ghosh, S. & Baltimore, D. Embryonic lethality and liver degeneration in mice lacking the RelA component of NF-κ B. *Nature* **376**, 167–170 (1995).
9. Li, Q., Van Antwerp, D., Mercurio, F., Lee, K.F. & Verma, I.M. Severe liver degeneration in mice lacking the IκB kinase 2 gene. *Science* **284**, 321–325 (1999).
10. Folli, F. *et al.* Regulation of endocytic-transcytotic pathways and bile secretion by phosphatidylinositol 3-kinase in rats. *Gastroenterology* **113**, 954–965 (1997).
11. Misra, S., Ujhazy, P., Gatmaitan, Z., Varticovski, L. & Arias, I.M. The role of phosphoinositide 3-kinase in taurocholate-induced trafficking of ATP-dependent canalicular transporters in rat liver. *J. Biol. Chem.* **273**, 26638–26644 (1998).
12. Misra, S., Ujhazy, P., Varticovski, L. & Arias, I.M. Phosphoinositide 3-kinase lipid products regulate ATP-dependent transport by sister of P-glycoprotein and multidrug resistance associated protein 2 in bile canalicular membrane vesicles. *Proc. Natl Acad. Sci. USA* **96**, 5814–5819 (1999).
13. Press, O.W., Press, N.O. & Kaufman, S.D. Evaluation and management of chylous ascites. *Ann. Intern. Med.* **96**, 358–364 (1982).
14. Jiang, B.H., Zheng, J.Z. & Vogt, P.K. An essential role of phosphatidylinositol 3-kinase in myogenic differentiation. *Proc. Natl Acad. Sci. USA* **95**, 14179–14183 (1998).
15. Shioi, T. *et al.* The conserved phosphoinositide 3-kinase pathway determines heart size in mice. *EMBO J.* **19**, 2537–2548 (2000).
16. Shepherd, P.R., Withers, D.J. & Siddle, K. Phosphoinositide 3-kinase: the key switch mechanism in insulin signalling. *Biochem. J.* **333**, 471–490 (1998).
17. Backer, J.M. *et al.* Phosphatidylinositol 3′-kinase is activated by association with IRS-1 during insulin stimulation. *EMBO J.* **11**, 3469–3479 (1992).
18. Shepherd, P.R. *et al.* Differential regulation of phosphoinositide 3-kinase adapter subunit variants by insulin in human skeletal muscle. *J. Biol. Chem.* **272**, 19000–19007 (1997).
19. Kerouz, N.J., Horsch, D., Pons, S. & Kahn, C.R. Differential regulation of insulin receptor substrates-1 and -2 (IRS-1 and IRS-2) and phosphatidylinositol 3-kinase isoforms in liver and muscle of the obese diabetic (ob/ob) mouse. *J. Clin. Invest.* **100**, 3164–3172 (1997).
20. Yu, J. *et al.* Regulation of the p85/p110 phosphatidylinositol 3′-kinase: stabilization and inhibition of the p110α catalytic subunit by the p85 regulatory subunit. *Mol. Cell. Biol.* **18**, 1379–1387 (1998).
21. Pons, S. *et al.* The structure and function of p55PIK reveal a new regulatory subunit for phosphatidylinositol 3-kinase. *Mol. Cell. Biol.* **15**, 4453–4465 (1995).
22. Franke, T.F., Kaplan, D.R. & Cantley, L.C. PI3K: downstream AKTion blocks apoptosis. *Cell* **88**, 435–437 (1997).
23. Sharma, P.M., Egawa, K., Gustafson, T.A., Martin, J.L. & Olefsky, J.M. Adenovirus-mediated overexpression of IRS-1 interacting domains abolishes insulin-stimulated mitogenesis without affecting glucose transport in 3T3-L1 adipocytes. *Mol. Cell. Biol.* **17**, 7386–7397 (1997).
24. Kim, Y.B. *et al.* Glucosamine infusion in rats rapidly impairs insulin stimulation of phosphoinositide 3-kinase but does not alter activation of Akt/protein kinase B in skeletal muscle. *Diabetes* **48**, 310–320 (1999).
25. Accili, D. *et al.* Early neonatal death in mice homozygous for a null allele of the insulin receptor gene. *Nature Genet.* **12**, 106–109 (1996).
26. Withers, D.J. *et al.* Disruption of IRS-2 causes type 2 diabetes in mice. *Nature* **391**, 900–904 (1998).
27. Egawa, K. *et al.* Membrane-targeted phosphatidylinositol 3-kinase mimics insulin actions and induces a state of cellular insulin resistance. *J. Biol. Chem.* **274**, 14306–14314 (1999).
28. Carpenter, C.L. *et al.* Purification and characterization of phosphoinositide 3-kinase from rat liver. *J. Biol. Chem.* **265**, 19704–19711 (1990).